Application of noninvasive functional imaging to monitor the progressive changes in kidney diffusion and perfusion in contrast-induced acute kidney injury rats at 3.0 T

Bin Zhang,[1,2] Yuhao Dong,[3] Baoliang Guo,[4] Wenbo Chen,[5] Fusheng Ouyang,[4] Zhouyang Lian,[3] Jing Liu,[3] Shuixing Zhang[1,2]

[1]Medical Imaging Center, First Affiliated Hospital of Jinan University, Guangzhou, People's Republic of China
[2]Institute of Molecular and Function Imaging, Jinan University, Guangzhou, People's Republic of China
[3]Department of Radiology, Guangdong General Hospital/Guangdong Academy of Medical Sciences, Guangzhou, Guangdong, People's Republic of China
[4]Department of Radiology, Shunde Hospital, Southern Medical University, Foshan, Guangdong, People's Republic of China
[5]Department of Radiology, Huizhou Municipal Central Hospital, Huizhou, People's Republic of China

Abstract

Objectives: Contrast-induced acute kidney injury is a prevalent cause of renal failure, and the noninvasive tools to monitor its progress are lacking. We applied intravoxel incoherent motion (IVIM) DWI to measure the progressive changes in kidney diffusion and perfusion of CI-AKI.
Methods: Twenty-four rats received Iopromide (370 mg/ml, 1600 mg iodine/kg) to induce CI-AKI. IVIM DWI was performed on rats ($n = 6$) at 24 h prior to and 12, 24, 48, 72, and 96 h after the injection using a 3.0 T MRI scanner. The progressive changes in the diffusion (D) and perfusion parameters (D^* and f) were studied in the cortex (CO), outer medulla (OM), and inner medulla (IM). For the histology group ($n = 18$), three rats were sacrificed at each time point.
Results: In the CO, D reduced progressively from 24 to 48 h ($P < 0.001$) and increased starting from 72 h ($P < 0.001$). However, D decreased until to 72 h in the medulla ($P < 0.001$) and increased starting from 96 h ($P < 0.001$). D^* decreased to the bottom at 24 h in the cortex and medulla ($P = 0.037$) and started to recover at 48 h ($P = 0.007$). f decreased in the cortex and medulla

in an early stage (12 h) ($P = 0.035$) of CI-AKI and then ascended in the later stage (72 h) ($P = 0.017$). The H & E staining showed different degrees of serial pathological change including cloudy swelling, atrophy, even necrosis, and interstitial vasodilation of tubule epithelial cells and glomerulus cells.
Conclusion: Our study demonstrates the feasibility of using IVIM DWI to monitor the progress of CI-AKI, implying that IVIM DWI is a useful biomarker in the staging of CI-AKI.

Key words: Intravoxel incoherent motion—DWI—Contrast-induced acute kidney injury

Contrast-induced acute kidney injury (CI-AKI) is a common iatrogenic event caused by the injection of iodinated contrast agent [1, 2] and remains the third major source of in-hospital acquired acute renal failure. It can cause long-term morbidity and mortality in elderly patients and patients with pre-existing kidney insufficiency or diabetes [3]. It is recognized now that the occurrence of CI-AKI is progressive, irreversible, and involves complex pathological changes, including hemodynamic alternation, medullary hypoxia, and direct cytotoxicity of contrast agents in the endothelial and renal tubular cells [4]. An iodinated contrast agent with high osmolality and viscosity is more likely to trigger the occurrence of CI-AKI.

Bin Zhang, Yuhao Dong, Wenbo Chen, and Baoliang Guo contributed equally to the work.

Correspondence to: Shuixing Zhang; *email:* shui7515@126.com

Currently, the diagnosis and grading of CI-AKI relies on the measurement of serum creatinine. Noninvasive imaging technologies that directly assess the kidney morphology and physiology can provide more accurate measurement of kidney function than serum creatinine and thus are highly desired. To date, a number of methods have been reported for the diagnosis and prognosis of kidney injury or dysfunction [5–8], either with or without the help of exogenous tracer (Gd-DTPA). The non-tracer-based approaches, such as diffusion-weighted imaging (DWI), arterial spin labeling (ASL), and blood oxygen level-dependent (BOLD) imaging, require no injection of imaging tracers, avoiding additional kidney burden, and hence can be used repeatedly and have wider applications. For example, DWI has been used to measure the damaged renal function, as quantified by apparent diffusion coefficient (ADC), caused by interstitial fibrosis or tubular atrophy [9, 10]. However, the accuracy of using DWI to measure kidney diffusion is questionable because ADC can be influenced not only by the changes in tissue and cellular structures, but also by the changes of the characteristics of local capillary network such as blood volume and blood flow [11]. ASL is a perfusion measuring MRI technology [12, 13] that has been applied to patients with acute kidney injury (AKI) [14, 15] and CI-AKI [16, 17]. However, ASL is limited by a relatively low signal-to-noise ratio (SNR) and is susceptible to motion artifacts. BOLD MRI technique is also useful to reveal changes in the oxygenation level in the injured kidney [17]. However, as was recently reported that changes in the blood oxygen level may not necessarily reflect the true changes in tissue pO2 [18], caution has to be taken in the interpretation of BOLD MRI for assessing the kidney function.

Recently, tremendous efforts have been made to implement intravoxel incoherent motion (IVIM) DWI technology to improve the DWI MRI detection or staging of many diseases including renal diseases. The advantage of IVIM DWI is its ability to separate the pure molecular diffusion (D) from the perfusion contribution, as characterized by the blood microcirculation volume fraction f and the perfusion-related diffusion D^*. As such, IVIM DWI is able to simultaneously detect both diffusion and perfusion characteristics of the tissue [19–23]. The purpose of this study is to examine the feasibility of using IVIM DWI to simultaneously measure the changes in kidney diffusion and perfusion in the course of CI-AKI, and to use it as an effective imaging tool to evaluate and stage kidneys undergoing CI-AKI.

Materials and methods

Animals

All procedures used in this study were approved by our Institutional Research Ethics Committee.

Twenty-four male Sprague-Dawley (SD) rats with body weights of 200–250 g were obtained from the provincial center, kept under standard conditions, and fed with standard rodent chow and free water. The CI-AKI was induced by tail vein injection of Iopromide (370 mg/ml, 2.22 g/kg body weight) [17].

MRI protocol

A total of six rats were imaged longitudinally at 24 h prior to the injection and at 12, 24, 48, 72, and 96 h after the injection of iodinated contrast agent. All MR imaging was performed on a 3.0 T whole-body system (Signa EXCITE HD, GE Healthcare, Milwaukee, WI) using a 40 mT/m, 200 mT/m/ms gradient system and a transmit birdcage body coil with 50 mm outer diameter. The rats were positioned as head first and supine so that the kidneys were aligned approximately with the center of the RF coil.

The IVIM DWI was performed using a single-shot diffusion-weighted spin-echo echo-planar sequence (coronal, TR/TE = 3000/73.6 ms, FOV = 10.0 × 10.0 cm, matrix = 96 × 96, NEX = 8, slice number = 3, slice thickness = 2.4 mm, intersection gap = 0.2 mm, total ten b values: 0, 20, 40, 60, 80, 100, 200, 400, 500, and 600 s/mm^2, scan time = 246 s). The lookup table of gradient directions was modified to allow multiple b value measurements in one series. A local shim box covering the kidney region was manually applied to minimize susceptibility artifacts.

Imaging processing

IVIM DWI

According to IVIM theory, the signal intensities and b values are related as follows:

$$S_b/S_0 = (1 - f) \cdot \exp(-b \cdot D) + f \cdot \exp(-b \cdot D*), \quad (1)$$

where S_0 is the signal intensity at $b = 0$, S_b is the signal intensity at nonzero b values, D is the true diffusion coefficient, D^* is the pseudo-diffusion coefficient due to microcirculation, and f is the microvascular volume fraction, i.e., the fraction of microcirculation in a given voxel. Because D^* is roughly one order of magnitude (10×10^{-3} mm^2/s) greater than $D - b \cdot D^*$ would be less than -4 at a high b value (> 200 s/mm^2), and $f \cdot \exp(-b \cdot D^*)$ would be less than $0.02 f$ in this study, therefore can be neglected. In this case, Eq. (1) can be simplified as follows:

$$S_b/S_0 = (1 - f) \cdot \exp(-b \cdot D). \quad (2)$$

Hence, high b values (400, 500, and 600 s/mm^2) were first fitted into Eq. (2) to calculate the D value. Although we had previously calculated the f value from Eq. (2), its accuracy was not acceptable, and therefore f should be

recalculated using Eq. (1). Then we fitted S_b for all b values into Eq. (1) with a fixed D value using a non-linear Levenberg–Marquardt method. When fitting Eq. (1), the initial estimated values for f and D^* were set to the f value calculated previously from Eq. (2) and 10×10^{-3} mm^2/s, respectively. Subsequently, the f and D^* values were obtained.

Data analysis

ADVANCE 4.3 Workstation software (General Electric Medical Systems) was used to analyze the IVIM images. To quantitatively compare the measurements between different time points and between different compartments of the kidney, we performed a region of interest (ROI) analysis of coronal IVIM images. We chose the right kidney only to reduce the potential cardiac- and lung-induced motion artifacts, which are larger in the left kidney than in the right. For each compartment, i.e., cortex (CO), outer medulla (OM), and inner medulla (IM), three representative ROIs of the upper, middle, and inferior regions were manually drawn on the T2-weighted anatomical image (T2WI) with the same shape and size (5 mm^2 and contained at least five pixels). The ROIs were placed to avoid the fatty tissues of the renal sinus and blood vessels. For each rat, the relative signal change (%) was calculated by comparing the calculated parameters at different post-injection times with that at 24 h before the injection of contrast medium (i.e., baseline).

Pathological analysis

The pathological images of H & E staining from the right kidney of rats were obtained at 24 h pre-injection and at 12, 24, 48, 72, and 96 h after the injection of contrast medium.

Statistical analysis

All results are reported as mean ± standard deviation (SD). All data were analyzed using SPSS 20.0 (SPSS Inc, Chicago, IL, USA). Two-way Repeated Measures AN-OVA and Least Significant Difference (LSD) method for further comparisons between specific group pairs were used. Two-tailed $P < 0.05$ was considered statistically significant.

Results

IVIM DWI

We acquired coronal oriented IVIM DWI images at ten different b values (0–600 s/mm^2) at a spatial resolution of 1.04×1.04 mm, which allows a clear visualization and separation of kidney structures, i.e., cortex (CO), outer

medulla (OM), and inner medulla (IM). The images were almost free of motion artifacts. Figure 1 shows the parametric maps of IVIM-metrics (including D, D^*, and f maps) at each time point. As shown in Fig. 2, bi-exponential IVIM model provides a good fitting in the CO, OM, and IM. Our results also showed a clearly higher baseline diffusion rate in the IM (1.83×10^{-3} mm^2/s) than that in the CO (1.74×10^{-3} mm^2/s) or OM (1.71×10^{-3} mm^2/s), which is consistent with previous reports [24].

Progressive changes of kidney diffusion in CI-AKI

To investigate the progressive changes in tissue diffusion in each part of the kidney during the course of CI-AKI, we performed a longitudinal DWI measurement for up to 96 h after the onset of CI-AKI. The calculated D values at each time point are listed in Table 1. When injected at a dose of 2.22 g/kg, the contrast medium Iopromide can cause a noticeable change in kidney diffusion at 12 h after the onset ($P < 0.001$). Specifically, as shown in Fig. 3 in the CO, the relative decrease of D ($\Delta D = (D^{pre} - D^t)/D^{pre} \times 100\%$) was 11.0% ($P < 0.0001$). The decrease in kidney diffusion first progressed with time and then reversed at around 48 h. The maximal decrease of the diffusion in the CO was at 48 h as compared to its baseline value, i.e., $\Delta D = 25.8\%$ ($P < 0.0001$). A similar pattern of decrease and recovery of tissue diffusion was observed in the OM and IM. Interestingly, the time to the maximal decrease in the medulla (72 h) is later than that in the cortex (48 h).

Progressive change of kidney perfusion in CI-AKI

The progressive changes of tissue perfusion in different parts of the kidney as measured by IVIM DWI (D^* and f) are shown in Table 1. Similar to the pattern of changes in tissue diffusion, all the perfusion-related parameters first decreased and then recovered. In particular, as shown in Fig. 4, the f values in both the cortex and medulla were markedly reduced (33.0%, 31.4%, and 39.0% for CO, IM, and OM, respectively) ($P = 0.000$–0.035) in the first 48 h, then recovered starting from 72 h ($P = 0.017$) and slowly back to 89.7%, 93.8%, and 96.3% of the baseline value by the end of MRI measurement (96 h) ($P = 0.179$). The D^* values were also markedly reduced (46.1%, 36.2%, and 42.1% for CO, IM, and OM, respectively) but reached their maximum at an earlier time point (i.e., 24 h) ($P = 0.037$), then recovered starting from 48 h ($P = 0.007$) and slowly back to 85.6%, 100.0%, and 78.5% of the baseline value by the end of MRI measurement (96 h) ($P = 0.333$).
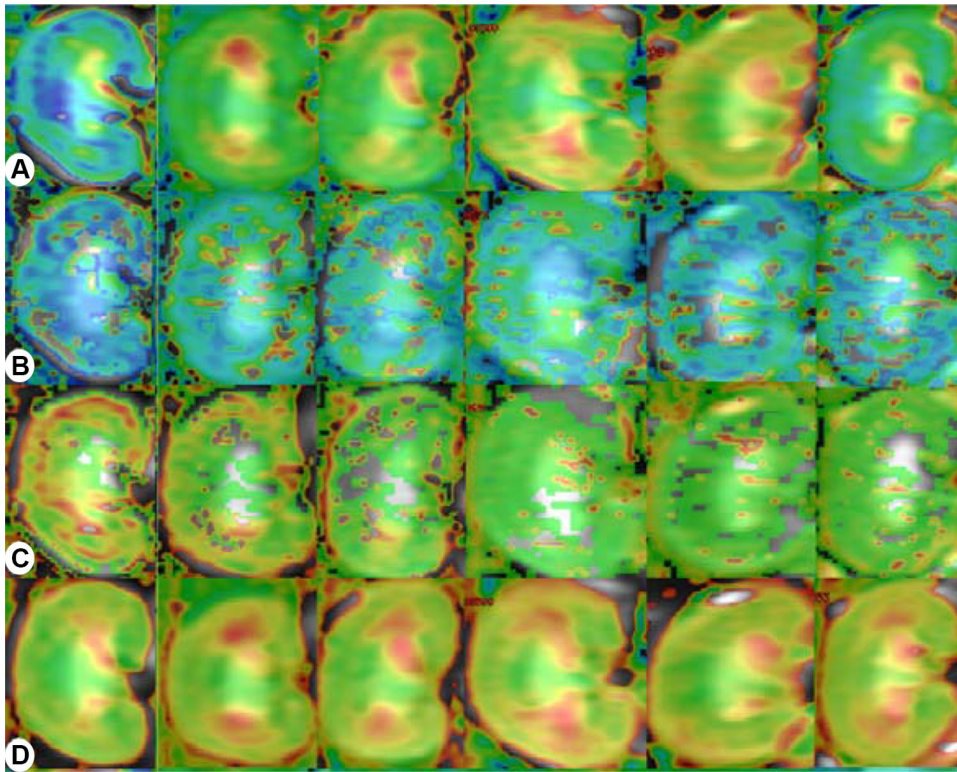
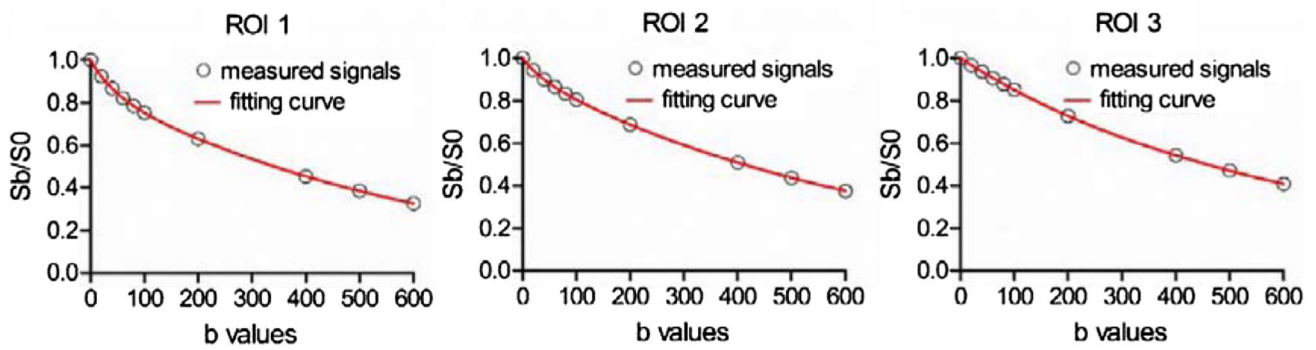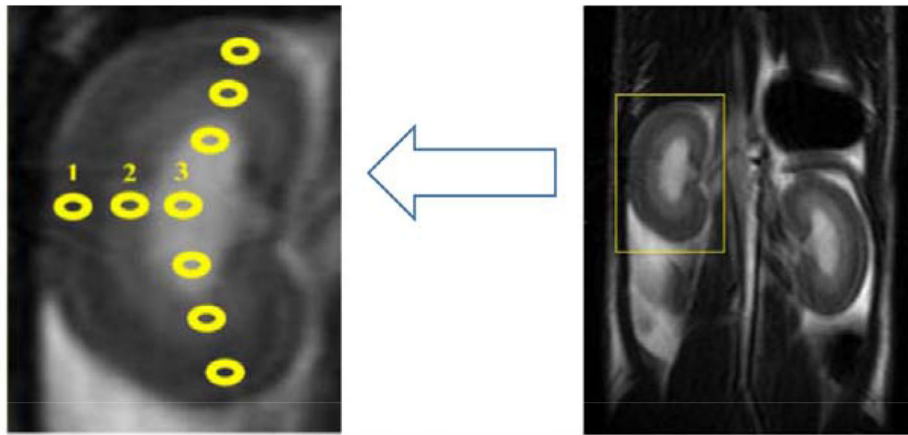**Fig. 1.** Parametric maps of IVIM-metrics (including D, D^*, and f maps) at each time point.

Fig. 2. IVIM bi-exponential model demonstrates the accuracy of data fitting. **A** A representative T2WI, on which nine ROIs were drawn in the *upper*, *middle*, and inferior regions of CO, OM, and IM, respectively, with the same shape and size (5 mm^2 and contained at least five pixels). ROI 1, ROI 2, and ROI 3 were placed at the same level of renal hilus. **B–D** Bi-exponential IVIM model provides a good fitting in the CO, OM, and IM.

Table 1. Mean D ($\times 10^{-3}$ mm^2/s), D^* ($\times 10^{-3}$ mm^2/s), and f (%) values at different time points during the course of CI-AKI ($n = 6$)

Parameter	Kidney tissue	Baseline	Post-injection				
			12 h	24 h	48 h	72 h	96 h
D	CO	1.63 ± 0.05	1.45 ± 0.06***	1.33 ± 0.06***	1.21 ± 0.04***	1.40 ± 0.06***	1.44 ± 0.05***
	OM	1.63 ± 0.05	1.48 ± 0.06***	1.38 ± 0.07***	1.29 ± 0.03***	1.24 ± 0.05***	1.44 ± 0.05***
	IM	1.74 ± 0.83	1.57 ± 0.59***	1.41 ± 0.88***	1.48 ± 0.79***	1.26 ± 0.67***	1.57 ± 0.76***
D^*	CO	36.9 ± 9.6	27.1 ± 0.75	19.9 ± 1.56*	21.2 ± 2.36**	27.6 ± 1.33*	31.6 ± 5.01
	OM	40.4 ± 14.14	27.7 ± 2.26	23.4 ± 1.93*	28.6 ± 1.46**	28.0 ± 1.35*	31.7 ± 1.68
	IM	37.3 ± 13.27	29.7 ± 8.80	23.8 ± 1.50*	25.7 ± 1.64**	30.0 ± 1.84*	37.7 ± 3.43
f	CO	29.1 ± 1.05	26.0 ± 1.55*	20.9 ± 1.80**	19.5 ± 2.13***	24.0 ± 1.93*	26.1 ± 4.91
	OM	29.8 ± 2.68	23.1 ± 1.94*	21.5 ± 1.93**	18.2 ± 1.79***	21.7 ± 1.76*	28.7 ± 2.20
	IM	30.6 ± 10.46	24.1 ± 11.74*	21.8 ± 1.45**	21.0 ± 1.92***	30.1 ± 1.85*	28.7 ± 1.96

Two-way Repeated Measures ANOVA and LSD method for further comparisons between specific group pairs
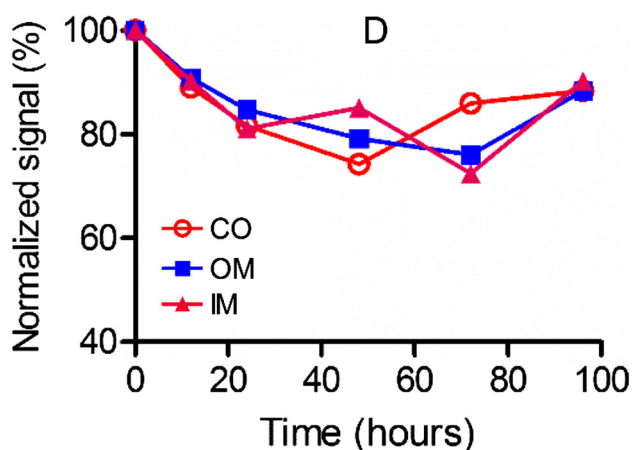All data are presented as the mean ± standard deviation (SD)
CI-AKI, contrast-induced acute kidney injury; CO, cortex; OM, outer medulla; IM, inner medulla
* $0.01 < P < 0.05$ (vs. baseline)
** $0.001 < P < 0.01$ (vs. baseline)
*** $P < 0.001$ (vs. baseline)
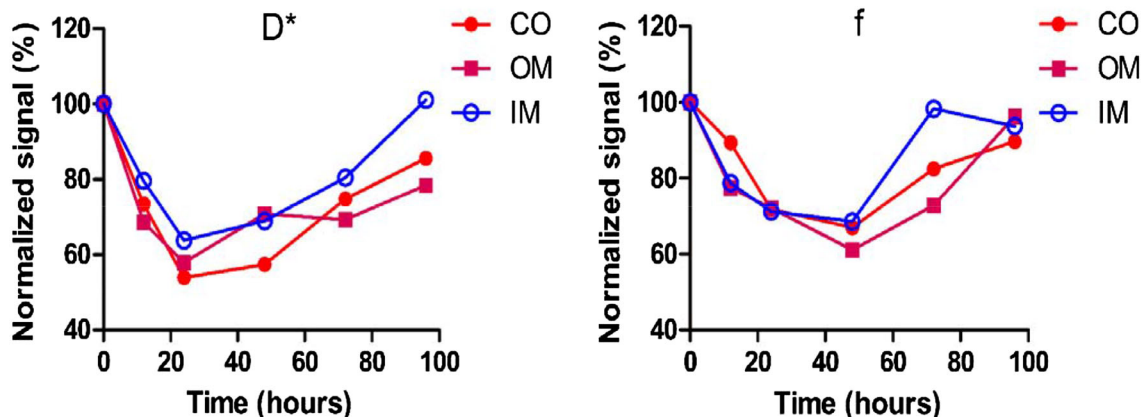

Fig. 3. Progressive change of tissue diffusion studied by IVIM DWI. The relative changes of D calculated by IVIM bi-exponential fitting at 24 h pre- (i.e., baseline) and 12, 24, 48, 72, and 96 h post-injection are shown for CO, OM, and IM.

The time course of perfusion and diffusion changes in different parts of the kidney throughout the progress of CI-AKI

We further compared the perfusion and diffusion changes in different parts of the kidney (Fig. 5a–c). The changes in D^* and D progressed at an almost identical pace in the CO, but not in the OM and IM. The change of D^* was similar in different parts of the kidney. All parameters significantly decreased in the first 12 h. D^* had the highest degree of signal change in the first 24 h (~42.5%) ($P = 0.037$). D^* is the most sensitive parameter that showed recovery as early as 24 h.

Evaluation of the pathological progress of CI-AKI using IVIM DWI

To determine whether we can use the perfusion and diffusion measured by IVIM DWI to evaluate the pro-

Fig. 4. Progressive change of tissue perfusion studied by IVIM DWI. The relative changes of D^* and f calculated by IVIM bi-exponential fitting at 24 h prior to the injection (i.e., baseline) and 12, 24, 48, 72, and 96 h post-injection are shown for CO (*red lines*), OM (*purple lines*), and IM (*blue lines*), respectively.
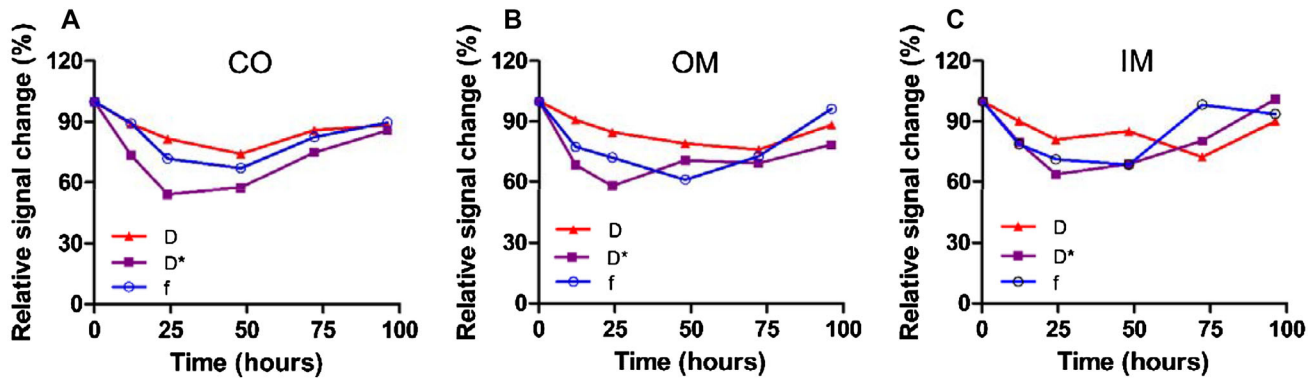
Fig. 5. IVIM measurement of the changes in kidney perfusion and diffusion in the progress of CI-AKI. The time course of **A** D (*green*), D* (*purple*), and f (*blue*) values in the CO; **B** D (*green*), D* (*purple*), and f (*blue*) values in the OM; and **C** D (*green*), D* (*purple*), and f (*blue*) values in the IM.

gress of CI-AKI, we performed the histological assessment of the kidney structures at different time points. The H & E staining (×400) clearly showed a progressive change in renal structure: at 12 h, a number of tubular epithelial cells were being broken down and part of the distal convoluted tubular lumens became narrow; at 24 h, small amounts swollen cells could be observed in glomerulus, but there was no sign of atrophy and fibrosis; at 48 h, there were both swollen cells and atrophy in glomerulus, and noticeable changes in part of proximal tubular and distal convoluted tubular epithelial cells (cloudy, swollen, fatty-degenerated, hyaline-degenerated, and necrotic); at 72 h, interstitial vasodilation started to be visible; finally, at 96 h, a small amount of interstitial vasodilation and congestion were observed. These histological findings are well correlated with the MRI findings at different times after the onset of CI-AKI (Fig. 6).

Discussion

As first demonstrated by Le Bihan et al. [11], the most commonly used quantitative metric, ADC, using in DWI, is indeed the combination of pure water diffusion (D) and the perfusion in microcirculation (i.e., D* and f), which can be separated using IVIM approach [25, 26]. Evidenced by numerous recently reported preclinical and clinical studies [19, 23, 27–29], IVIM DWI can provide aim-proved interpretation of DWI data. Our study shows the application of IVIM DWI in the assessment of the renal pathophysiological processes in CI-AKI.

Our data indicated that D values are slightly larger in the IM (1.74×10^{-3} mm^2/s) than those in the CO and OM (1.63 and 1.63×10^{-3} mm^2/s, respectively) at 24 h prior to the injection. Our data also indirectly confirm that the change in kidney diffusion can be used as an indicator of kidney function [30]. Interestingly, the maximum decrease in D value occurred at 48 and 72 h in the cortex and medulla, respectively, suggesting that the damaged cells in

the cortex can recover quicker than those in the medulla after injury, in good agreement with the previous report in rabbit model [31]. The change of kidney diffusion can be explained by the change in both intracellular water (i.e., swollen cells in the proximal convoluted tubule and glomerulus) and intrarenal water, due to the fact that Iopromide has a much higher osmolarity than that of blood plasma [32]. This decrease in water diffusivity during CI-AKI may be also further deteriorated by decreased tissue pO2 as a result of impaired blood supply, which makes tubular cells more vulnerable [33].

Compared to conventional DWI, IVIM DWI is inherently capable of simultaneously assessing both diffusion and perfusion during the progress of CI-AKI. In particular, D* has been shown to be sensitive to vascular blood [34, 35], whereas f is the ratio of vascular and tubular fluid volume to the total fluid in the tissue (i.e., intrarenal water contents) [19].

Our findings show that starting from 12 h post-injection, with the progress of CI-AKI, significant decreases of other perfusion-related parameters could be observed, suggesting the decrease of cortical and medullary fluid volume (i.e., f) as a result of tubuloglomerular response to vasoconstriction. Interestingly, we found that the time point for D* to recover (i.e., 24 h) was earlier than f, which may be due to the fact that vasodilation occurred also slightly earlier than the recovery of capillary blood volume [19] and blood flow [18]. In contrast to the recovery of tissue diffusion, perfusion-related parameters recovered back more nearly to the level of pre-injection, which is likely due to the compensatory mechanism that can increase arterial pressure, tubular flow, and hyperfiltration [17]. The longitudinal study thus proved that, while f and D* are perfusion-related parameters, they are sensitive to different pathological changes in the course of CI-AKI, and thus are complementary, indicating that a comprehensive evaluation of f and D* may provide more accurate diagnosis of disease progress.
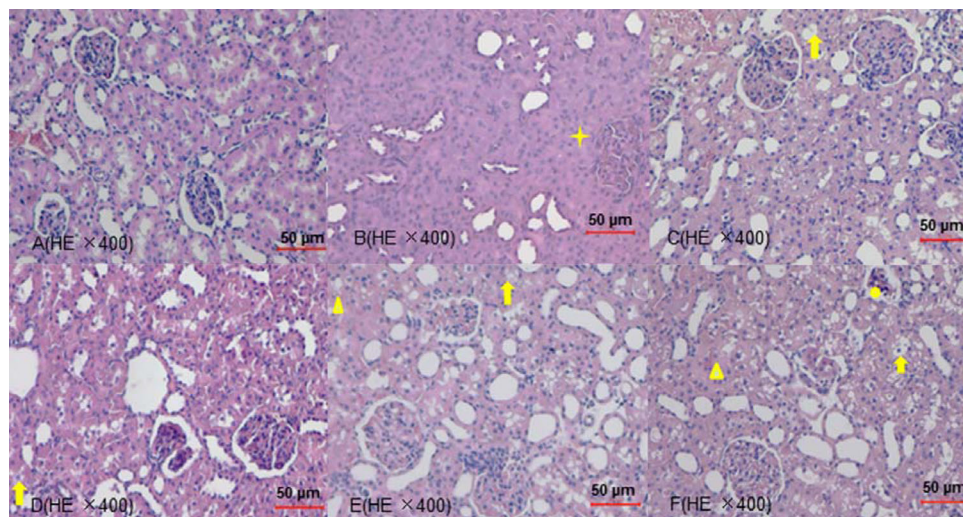
Fig. 6. Representative H & E-stained histological sections of the kidneys at each time point throughout the course of CI-AKI: **A** 24 h prior to the injection, **B** 12 h after the injection, **C** 24 h after the injection, **D** 48 h after the injection, **E** 72 h after the injection, and **F** 96 h after the injection. Different degrees of serial patho- logical change including cloudy swelling, atrophy, even necrosis, and interstitial vasodilation of tubule epithelial cells and glomerular cells. *Note*: four-horn star represents swollen cell, triangle represents interstitial congestion, arrow represents fatty-degenerated cell, and seven-horn star represents atrophy.

The study has some limitations. First, the quantitative comparisons were performed using the mean values of a number of manually drawn ROIs in different parts of the kidney or at different locations of the same parts, which makes our analysis prone to error. In the future, an automatic tissue segmentation technique should be used to reduce the potential bias and error caused by ROI drawing. In addition, while a relatively large animal volume ($n = 6$ for MRI and $n = 3$ for histology at each time point) was used, the histologic evaluation was not performed on the same individual animal that underwent MRI assessments. Because each individual animal may have different responses to the injection of iodinated agents, it would be ideal if the histology is performed on the same animal after each MRI session, which, however, is difficult. Finally, our analysis was performed on a single kidney (i.e., the right kidney) by assuming that both kidneys have the identical response to the injected iodinated agent. Including both kidneys may improve the accuracy of our study.

In conclusion, our study demonstrates the feasibility of using IVIM DWI to monitor the progress of CI-AKI in an animal model, implying that IVIM DWI is a useful biomarker in the diagnosis and staging of CI-AKI. Considering that IVIM DWI technique has been implemented in the clinical regimes, our approach can be quickly translated to the patient study for monitoring renal pathophysiologic alternations after the administration of iodinated contrast medium, which will greatly benefit elderly patients or patients with pre-existing kidney insufficiency and diabetes.

References

1. Wessely R, Koppara T, Bradaric C, et al. (2009) Choice of contrast medium in patients with impaired renal function undergoing percutaneous coronary intervention. Circ Cardiovasc Interv 2:430–437
2. Kodama A, Watanabe H, Tanaka R, et al. (2013) A human serum albumin-thioredoxin fusion protein prevents experimental contrast-induced nephropathy. Kidney Int 83:446–454
3. Abu JB, Kanso AA, Schelling JR (2009) Evidence-based approach for prevention of radiocontrast-induced nephropathy. J Hosp Med 4:500–506
4. Haller C, Hizoh I (2004) The cytotoxicity of iodinated radiocontrast agents on renal cells in vitro. Invest Radiol 39:149–154
5. Notohamiprodjo M, Reiser MF, Sourbron SP (2010) Diffusion and perfusion of the kidney. Eur J Radiol 76:337–347
6. Zhang JL, Morrell G, Rusinek H, et al. (2014) New magnetic resonance imaging methods in nephrology. Kidney Int 85:768–778
7. Notohamiprodjo M, Kalnins A, Andrassy M, et al. (2016) Multiparametric functional MRI: a tool to uncover subtle changes following allogeneic renal transplantation. PLoS One 11:e165532
8. Hueper K, Gutberlet M, Brasen JH, et al. (2016) Multiparametric functional MRI: non-invasive imaging of inflammation and edema formation after kidney transplantation in mice. PLoS One 11:e162705
9. Yildirim E, Kirbas I, Teksam M, et al. (2008) Diffusion-weighted MR imaging of kidneys in renal artery stenosis. Eur J Radiol 65:148–153
10. Togao O, Doi S, Kuroo M, Masaki T, Yorioka N (2010) Assessment of renal fibrosis with diffusion-weighted MR imaging: study

with murine model of unilateral ureteral obstruction. Radiology 255:772–780

11. Le Bihan D, Breton E, Lallemand D, et al. (1988) Separation of diffusion and perfusion in intravoxel incoherent motion MR imaging. Radiology 168:497–505

12. Bivard A, Krishnamurthy V, Stanwell P, et al. (2014) Arterial spin labeling versus bolus-tracking perfusion in hyperacute stroke. Stroke 45:127–133

13. Lanzman RS, Robson PM, Sun MR, et al. (2012) Arterial spin-labeling MR imaging of renal masses: correlation with histopathologic findings. Radiology 265:799–808

14. Heusch P, Wittsack HJ, Heusner T, et al. (2013) Correlation of biexponential diffusion parameters with arterial spin-labeling perfusion MRI: results in transplanted kidneys. Invest Radiol 48:140–144

15. Zimmer F, Zollner FG, Hoeger S, et al. (2013) Quantitative renal perfusion measurements in a rat model of acute kidney injury at 3T: testing inter- and intramethodical significance of ASL and DCE-MRI. PLoS One 8:e53849

16. Liu YP, Song R, Liang C, Chen X, Liu B (2012) Arterial spin labeling blood flow magnetic resonance imaging for evaluation of renal injury. Am J Physiol Renal Physiol 303:F551–F558

17. Zhang Y, Wang J, Yang X, et al. (2012) The serial effect of iodinated contrast media on renal hemodynamics and oxygenation as evaluated by ASL and BOLD MRI. Contrast Media Mol Imaging 7:418–425

18. Leong CL, Anderson WP, O'Connor PM, Evans RG (2007) Evidence that renal arterial-venous oxygen shunting contributes to dynamic regulation of renal oxygenation. Am J Physiol Renal Physiol 292:F1726–F1733

19. Sigmund EE, Vivier PH, Sui D, et al. (2012) Intravoxel incoherent motion and diffusion-tensor imaging in renal tissue under hydration and furosemide flow challenges. Radiology 263:758–769

20. Ichikawa S, Motosugi U, Ichikawa T, et al. (2013) Intravoxel incoherent motion imaging of the kidney: alterations in diffusion and perfusion in patients with renal dysfunction. Magn Reson Imaging 31:414–417

21. Jerome NP, Orton MR, D'Arcy JA, et al. (2014) Comparison of free-breathing with navigator-controlled acquisition regimes in abdominal diffusion-weighted magnetic resonance images: effect on ADC and IVIM statistics. J Magn Reson Imaging 39:235–240

22. Rheinheimer S, Schneider F, Stieltjes B, et al. (2012) IVIM-DWI of transplanted kidneys: reduced diffusion and perfusion dependent on cold ischemia time. Eur J Radiol 81:e951–e956

23. Chandarana H, Lee VS, Hecht E, Taouli B, Sigmund EE (2011) Comparison of biexponential and monoexponential model of diffusion weighted imaging in evaluation of renal lesions: preliminary experience. Invest Radiol 46:285–291

24. Notohamiprodjo M, Chandarana H, Mikheev A, et al. (2015) Combined intravoxel incoherent motion and diffusion tensor imaging of renal diffusion and flow anisotropy. Magn Reson Med 73:1526–1532

25. Federau C, Sumer S, Becce F, et al. (2014) Intravoxel incoherent motion perfusion imaging in acute stroke: initial clinical experience. Neuroradiology 56:629–635

26. Joo I, Lee JM, Han JK, Choi BI (2014) Intravoxel incoherent motion diffusion-weighted MR imaging for monitoring the therapeutic efficacy of the vascular disrupting agent CKD-516 in rabbit VX2 liver tumors. Radiology 272:417–426

27. Patel J, Sigmund EE, Rusinek H, et al. (2010) Diagnosis of cirrhosis with intravoxel incoherent motion diffusion MRI and dynamic contrast-enhanced MRI alone and in combination: preliminary experience. J Magn Reson Imaging 31:589–600

28. Zhang SX, Jia QJ, Zhang ZP, et al. (2014) Intravoxel incoherent motion MRI: emerging applications for nasopharyngeal carcinoma at the primary site. Eur Radiol 24:1998–2004

29. Luciani A, Vignaud A, Cavet M, et al. (2008) Liver cirrhosis: intravoxel incoherent motion MR imaging–pilot study. Radiology 249:891–899

30. Persson PB, Hansell P, Liss P (2005) Pathophysiology of contrast medium-induced nephropathy. Kidney Int 68:14–22

31. Wang J, Zhang Y, Yang X, et al. (2012) Time course study on the effects of iodinated contrast medium on intrarenal water transport function using diffusion-weighted MRI. J Magn Reson Imaging 35:1139–1144

32. Messenger JC, Casserly IP (2009) Advances in contrast media and contrast injectors. Cardiol Clin 27:407–415

33. Ari E, Kedrah AE, Alahdab Y, et al. (2012) Antioxidant and renoprotective effects of paricalcitol on experimental contrast-induced nephropathy model. Br J Radiol 85:1038–1043

34. Chandarana H, Kang SK, Wong S, et al. (2012) Diffusion-weighted intravoxel incoherent motion imaging of renal tumors with histopathologic correlation. Invest Radiol 47:688–696

35. Thoeny HC, De Keyzer F, Oyen RH, Peeters RR (2005) Diffusion-weighted MR imaging of kidneys in healthy volunteers and patients with parenchymal diseases: initial experience. Radiology 235:911–917